COMPDYN 2025
10th ECCOMAS Thematic Conference on
Computational Methods in Structural Dynamics and Earthquake Engineering
M. Papadrakakis, M. Fragiadakis (eds.)
Rhodes Island, Greece, 15-18 June 2025

LIFE CYCLE IMPACT REDUCTION ALLOWED BY SEISMIC REHABILITATION OF PRECAST CONCRETE STRUCTURES

Margherita Buttazzoni[1], Martina Caruso[2], Francesco Cavalieri[3*], Davide Bellotti[3] and Roberto Nascimbene[1,3]

[1] *University School for Advanced Studies (IUSS), Department of Science, Technology and Society*
Palazzo del Broletto, Piazza della Vittoria 15, 27100, Pavia, Italy
Email: margherita.buttazzoni@iusspavia.it, roberto.nascimbene@iusspavia.it

[2] *Global Earthquake Model (GEM), Via Adolfo Ferrata 1, 27100, Pavia, Italy*
Email: martina.caruso@globalquakemodel.org

[3] *European Centre for Training and Research in Earthquake Engineering (EUCENTRE)*
Via Adolfo Ferrata 1, 27100, Pavia, Italy
Email: francesco.cavalieri@eucentre.it, davide.bellotti@eucentre.it, roberto.nascimbene@eucentre.it

Abstract

Sustainability issues related to seismic retrofit of precast structures have been so far disregarded or not fully explored. Building on recent research that quantitatively assesses the environmental impact of traditional and dissipation-based retrofitting strategies, this paper aims to bridge this gap by evaluating their potential to reduce building earthquake-induced economic and environmental impacts. Two alternative strategies, entailing concrete jacketing of columns and the use of two energy dissipation devices, respectively, were designed for the retrofit of a single-storey precast industrial building, typical of the '70s Italian construction practice. The FEMA P-58 component-based approach was adopted for the seismic loss assessment of the structure in its as-built and post-retrofit configurations, through the employment of the PACT tool. The evaluation of the building structural performance under seismic loads was conducted by subjecting the 3D numerical models created in OpenSees to a number of nonlinear dynamic analyses. Comparing seismic repair costs and equivalent carbon emissions, a substantial impact reduction was observed in both retrofitted configurations, especially concerning costs. Such reduction is more pronounced, under a life cycle perspective, for the innovative dissipation-based solution, thus confirming its great potential if compared to the more traditional concrete jacketing of columns.

Keywords: Friction rotation damper, Braces, Multiple-stripe analysis (MSA), Life cycle assessment (LCA), Seismic loss assessment

1 INTRODUCTION

Following the recent earthquakes that struck Italy, namely Abruzzo 2009, Emilia-Romagna 2012 and Central Italy 2016–2017 (see e.g. Praticò et al., 2022 [1]), reinforced concrete (RC) precast industrial buildings suffered extensive damage. For structures not specifically designed to resist lateral loads, seismic rehabilitation is particularly crucial to extend their nominal service life and help reduce the potential seismic losses. Traditional retrofitting techniques include concrete or steel jacketing of structural members, as well as fibre reinforced polymers (FRP) or high-performance fibre reinforced concrete (HPFRC) wrapping. Li et al. (2020) [2] investigated, through reversed-cyclic lateral loading tests, the seismic performance of a precast wall system retrofitted with steel jacketing for confinement of the wall base, coupled with replaceable, external buckling restrained plates (BRPs) for energy dissipation. This reflects how innovative, dissipation-based solutions are being increasingly used in recent years as alternatives to traditional retrofitting techniques, in an effort to enhance the seismic response of precast structures.

Indeed, the latest decades observed increasing scientific research efforts devoted to the development and application of devices that impose the dissipation of an appropriate amount of energy, thus helping protect the structural members. Such devices typically dissipate energy through friction or by material hysteresis and may be combined with elements having the function to increase the initial stiffness; in this way, they prevent or mitigate the second order effects and avoid excessive displacements at the serviceability limit state.

In this context, the focus in this work is on dissipative devices designed for beam-to-column connections of precast industrial buildings, as well as dissipative bracing systems. To date, the latter have been only partially investigated, e.g., by Guerrero et al. (2018) [3] and Dal Lago et al. (2021) [4]. On the other hand, a number of retrofitting solutions that are applicable to frictional or dowel-based beam-to-column connections have been proposed. Several works investigated the dissipation capabilities of a friction rotation damper, with and without the addition of a re-centring device (e.g. Santagati et al., 2012 [5] and Belleri et al., 2017 [6]), and a hysteretic rotation damper (Javidan et al., 2022) [7]. Sonda and Pollini, 2023 [8] quantified the performance enhancement attained by precast structures equipped with dissipative fuse devices, patented with the name of Sismocell, at beam-to-column joints. Magliulo et al. (2017) [9] investigated the shear strength of a new retrofitting system consisting of a three-hinged steel device through two cyclic tests on a damaged beam-to-column dowel-based connection.

From a sustainability perspective, it is already known that seismic rehabilitation techniques i) naturally carry their own life cycle environmental impact, and ii) aim to mitigate earthquake-induced losses, thus reducing contextually economic, environmental and social life cycle impacts of existing buildings. These relevant aspects have traditionally been neglected or only partially considered, in general and specifically for precast structures. Passoni et al. (2022) [10] recently discussed a new, holistic viewpoint of the problem, by redefining the life cycle thinking (LCT) principles and targets that can be adopted in the design of retrofitting techniques to control their life cycle impacts (including, e.g., repairability, durability, flexibility and adaptability, and deconstruction). In addition, to identify optimal retrofitting strategies, several multi-criteria decision-making (MCDM) approaches have been proposed for buildings, including a range of economic, social, technical, and, more recently, environmental criteria that are assumed to be of interest to decision-makers (e.g. Caruso et al., 2023 [11], Clemett et al., 2023 [12], Giresini et al., 2021 [13]). A few other research works are available in the literature that carry out life cycle assessment (LCA) of structural/seismic retrofitting techniques for existing buildings, but none of them explored retrofitting measures for precast structures.

Building on recent research by the authors (Cavalieri et al., 2023) [14] that quantitatively assesses the environmental impact of traditional and dissipation-based retrofitting strategies for

precast structures, the goal of this work is to investigate the potential reduction of earthquake-induced economic and environmental impacts offered by such retrofitting strategies. With reference to a single-storey RC precast building, a comparative evaluation of seismic repair costs and equivalent carbon emissions was undertaken on the building in its as-built configuration and retrofitted with two alternative solutions: in the first (traditional) one, RC jacketing of columns was used, whilst in the second (innovative) one, two energy dissipation devices were jointly employed, namely a friction rotation damper for beam-to-column connections and a bracing system with dissipative sacrificial elements. In the final part of the manuscript, the economic and environmental costs of both retrofitting solutions are also accounted for, to allow for a more significant comparison of such techniques under a life cycle perspective.

2 CASE STUDY BUILDING AND PROPOSED RETROFITTING SOLUTIONS

The case study considered for this endeavour, depicted in Figure 1 and already studied in [14], is a single-storey precast structure representative of the Italian construction period of the '70s, located in Naples on soil type C and designed on the base of gravity loads only. The geometry consists of a single span with total plan size of 20 × 54 m^2, with ten portal frames in the transverse (x) direction. The columns are characterised by a 0.35 × 0.35 m^2 cross-sectional area and a 6 m height. The ten prestressed main beams in the transverse direction feature a span length of 20 m, a double slope of 10% inclination, and an I-section with variable height and web thickness. The connections of the main beams to the columns only rely on friction and are characterised by the presence of neoprene pads on the column top allowing for beam seating. The roof is composed of double-tee prestressed elements, rigidly fastened to the main beams by reinforcement stirrups protruding from the beams. The external closure, which is present on all sides of the building, is made up of masonry infill panels constituted of hollow bricks of the type called Italian "double-UNI", creating ribbon windows of a 1.5 m height; the upper part of the column, adjacent to ribbon windows, is called short or squat column hereafter.

The building does not satisfy the current Italian seismic code provisions, namely NTC18 [15], even just for the presence of friction-based connections. It was then decided herein to apply two rehabilitation techniques, respectively of traditional and innovative type, which allow the structure to withstand the seismic demands prescribed by the code for new constructions, at the life safety limit state.

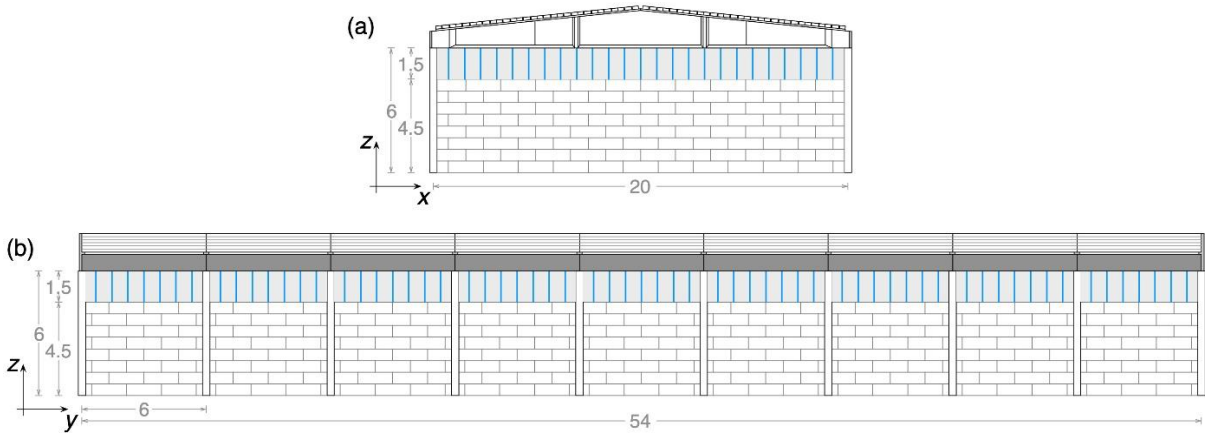

Figure 1: (a) Frontal and (b) side view of the case study building (Units: m).

Starting with RC jacketing of columns, it was decided to use a class C28/35 concrete for the column jackets, and steel of class B450C for the new rebars. A jacket with a 10 cm thickness was added along all sides of existing columns, resulting in a 0.55 × 0.55 m^2 cross-sectional area,

with a longitudinal reinforcement of 20 ϕ14 mm rebars (see Figure 2a), corresponding to the minimum reinforcement ratio of 1%. The implementation of column jacketing also required i) the removal of infill portions adjacent to columns, for a 50 cm width, ii) their replacement, after the intervention, with the same brick type for a 25 cm width plus a 15 cm wide finishing mortar casting, as well as iii) the replacement of ribbon windows along the whole perimeter of the building. Concrete jacketing was also coupled with the application, at beam-to-column frictional connections, of UPN300 commercial steel profiles and passing holes hosting ϕ24 mm steel pins, which allow for relative rotations but prevent joint sliding. Two profiles for each end of the main beams were introduced, for a total of 10 × 4 = 40 profiles. Such profiles are attached to the columns by a total of eight ϕ20 mm fasteners, arranged into four rows (see Figure 2b).

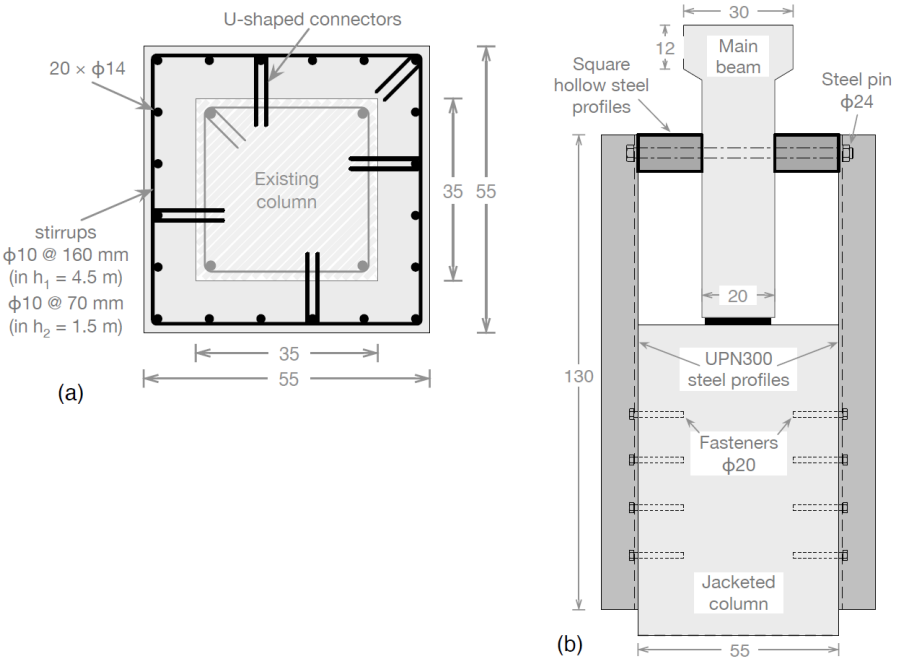

Figure 2: (a) Cross-section of the jacketed column (note that h1 and h2 are the heights of the lower and upper squat part of the column, respectively), and (b) frontal view of a beam-to-column frictional connection, with UPN300 steel profiles and spacers applied to prevent joint sliding (Units: cm, unless otherwise specified).

Coming to the dissipative devices considered herein, the first one is a friction rotation damper (see Figure 3a), conceived to be applied at beam-to-column connections. The device is able to dissipate energy (thus increasing the system damping) through the friction generated by the relative rotation of steel plates with interposed brass discs. It was assumed that interposing four brass discs yields an activation moment of 40 kNm, a value selected for this application among the three values considered by Santagati et al. (2012) [5], namely 40, 80 and 120 kNm. The device works in a three-hinge scheme, where sliding surfaces are applied only at one hinge, whilst the remaining two hinges are left free to rotate. It was decided to install the rotation dampers only at the beam-to-column frictional connections in the ten portal frames that include the main beams, along the transverse direction: this choice entailed the introduction of a total of 10 × 2 = 20 rotation dampers. To avoid joint sliding, the rotation dampers were coupled with UPN200 commercial steel profiles and passing holes hosting ϕ24 mm steel pins.

The second dissipative device adopted in this work entails the use of non-traditional diagonal steel braces, characterised by the inclusion of dissipative sacrificial elements, as well as the presence of a junction in the middle, which allows the upper and lower portions of the braces to be off-axis (Resilio system, 2017) [16]. This system is able to channel the ingoing seismic

energy towards predefined points in the vicinity of the junction, where the steel sacrificial elements are located (see Figure 3b). The latter, which for this application are made of 60 × 4 mm S355 steel lamellas (class 60), are pushed in the nonlinear field and dissipate energy by material hysteresis of steel, thus preserving the rest of the structure. The braces were installed only along the longitudinal direction, within the central bay of the perimeter portal frames. The lower and upper portions of the braces are herein constituted by HEA200 profiles and square hollow profiles, respectively, both with S275 steel.

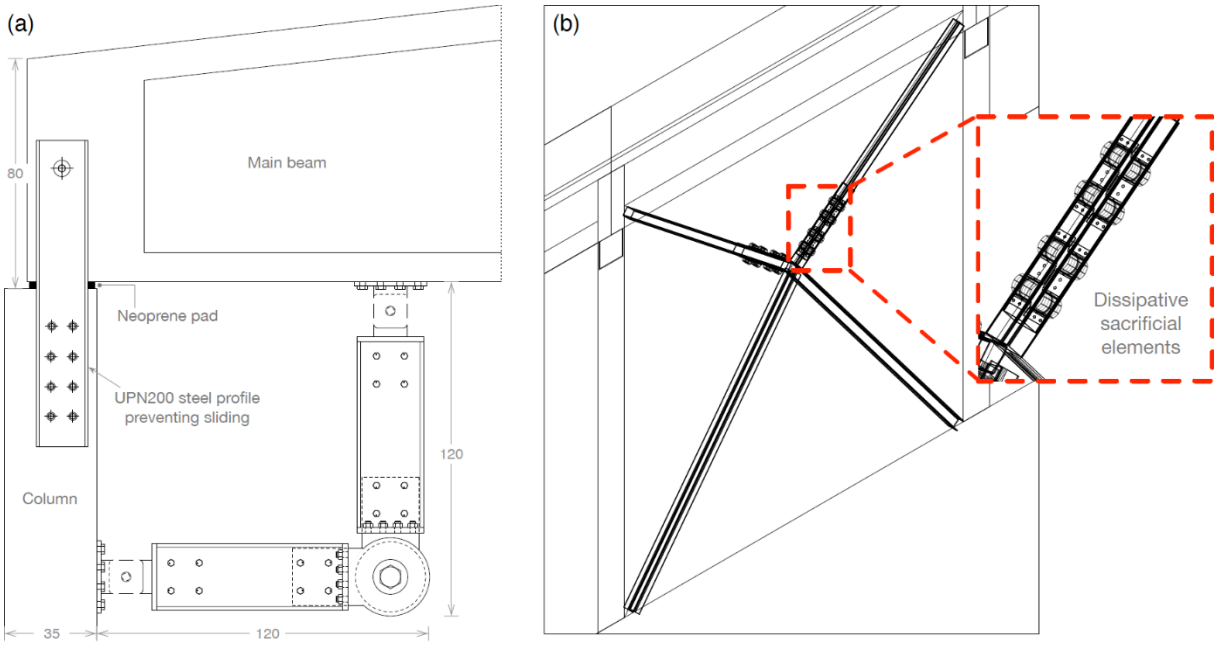

Figure 3: (a) Side section detail of the adopted friction rotation damper applied at beam-to-column connections, and (b) axonometric view of the diagonal steel braces (Units: cm).

3 STRUCTURAL PERFORMANCE ASSESSMENT

In Cavalieri et al. (2023) [14], three 3D numerical models of the case study building were created in OpenSees (McKenna et al., 2000) [17] to investigate its seismic response before and after the retrofit. The first model, named M1 hereafter, reflects the unretrofitted, as-built configuration, whilst the remaining two models represent the building as retrofitted with RC jacketing (model M2) and both dissipation-based devices (model M3). Due to space constraints, the modelling assumptions are not reported here, and can be found in [14].

This Section briefly presents the results of a research work carried out within the Italian project RINTC (2022-2024) [18], concerning in particular the nonlinear dynamic analyses executed on the three models in a multiple-stripe analysis (MSA) framework (Jalayer and Cornell, 2009) [19]. For all three models, based on their fundamental periods T_1, the same conditioning intensity measure (IM) was adopted, namely the spectral acceleration $S_a(T_1)$ at $T_1 = 0.5$ s. Ten increasing IM levels (IML) of $S_a(0.5)$ were considered within MSA: at each of them, both horizontal components of 20 natural spectrum-compatible recordings were extracted from the Engineering Strong Motion (ESM) database (Luzi et al., 2020) [20].

For the unretrofitted model, two engineering demand parameters (EDPs) were evaluated in the dynamic analyses. The first one is the maximum (in time) absolute value of the column drift among the two horizontal directions, whilst the second one is the maximum (in time) absolute value of the relative displacement of the beam-to-column frictional connections, among the two horizontal directions. For the retrofitted models, only the first EDP was evaluated, given that

joint sliding is prevented. The dynamic response was assessed with reference to two limit states, namely the Usability Preventing Damage (UPD) and the Global Collapse (GC).

Figure 4 displays the highest demand-over-capacity (D/C) ratio points, limited to 1, obtained among the two horizontal directions and the two EDPs evaluated, and resulting from MSA at both limit states. The D/C median curves are also displayed. The plots show a significant reduction of seismic demands for both the retrofitted models at both limit states. At GC, it can be noted how the divergence of the blue and green median curves increases with seismic intensity, reflecting an increase in energy dissipation for model M3, as expected. Overall, these results do provide reassurance on the efficacy of both the traditional and dissipation-based retrofitting solutions in effectively yielding a performance enhancement for the case study at hand.

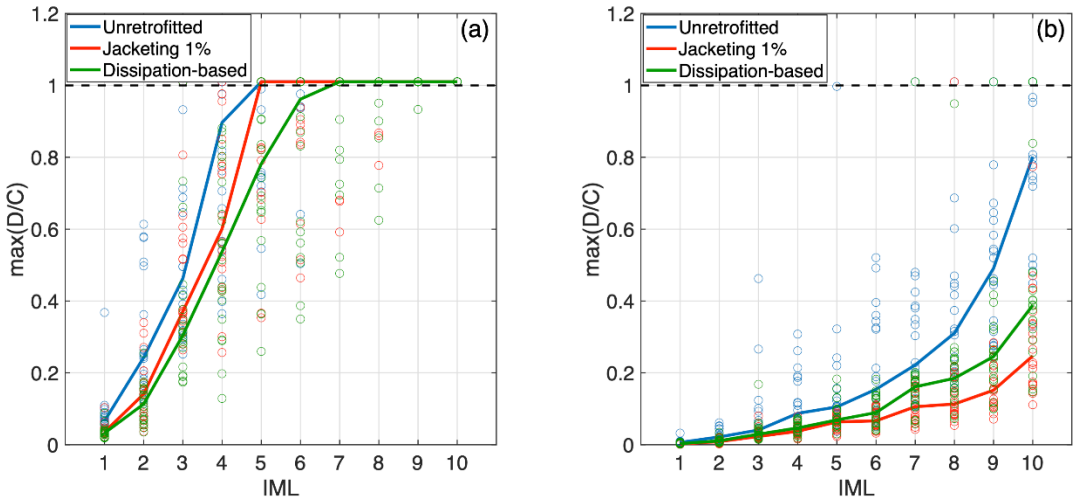

Figure 4: D/C ratio points and median curves obtained via MSA for the three investigated models, at the (a) UPD limit state, and (b) GC limit state.

4 ECONOMIC AND ENVIRONMENTAL SEISMIC LOSS ASSESSMENT OF AS-BUILT AND RETROFITTED CONFIGURATIONS

The as-built configuration and both retrofitting solutions were compared by carrying out the assessment of seismic losses in economic and environmental terms, i.e. quantifying the Average Annual Loss (AAL) and the Average Annual Embodied Carbon (AAEC) as measures of the economic and environmental costs associated with repair and reconstruction activities following seismic events. The FEMA P-58 probabilistic approach for seismic loss assessment (ATC, 2018a,b [21][22]) was adopted, consisting of the following steps: (i) seismic hazard quantification at the site (the latter being reported in Section 2), (ii) structural performance analysis under seismic loads (described in Section 3), (iii) estimation of damage level of building's vulnerable components, and (iv) calculation of losses due to repair of damaged components or building replacement after collapse or non-repairable scenarios.

A fundamental step (step iii) of the seismic loss assessment procedure is the creation of the inventory of vulnerable structural and nonstructural building's components, which are expected to experience damage during an earthquake. Each of these components features a fragility function and a set of consequence functions. Fragility functions indicate the conditional probability of reaching a damage state (DS) given a certain value of seismic demand, expressed in terms of an EDP, e.g. inter-storey drift ratio, peak floor acceleration or velocity. Consequence functions are instead used to translate each damage state into potential repair costs, repair time, repair embodied carbon, fatalities etc.

The vulnerable components included in the inventories of the as-built and concrete jacketing configurations are the following: (i) RC brittle weak columns (BWCs) (Cardone, 2016) [23] and (ii) exterior masonry infills without windows, with expected out-of-plane collapse mechanism (EIWs) (Cardone and Perrone, 2015) [24]. Brittle columns were used to consider the short columns in correspondence of ribbon windows, and counted per piece in both *x* and *y* directions. External infills were instead measured per unit area in both *x* and *y* directions, with their collapse damage state assumed to occur out-of-plane. Fragility and repair cost functions developed in Refs. [23] and [24] for those components, specifically for Italian and European RC frame buildings built before the 70s, were used. Repair costs, originally estimated according to 2013 Italian price list [23][24], were updated to 2024 prices by using an inflation factor equal to 1.28. The consequence functions in terms of embodied carbon for these components were instead taken from Ref. [11]. For the jacketed configuration, environmental consequence functions of brittle columns were increased with respect to those of the as-built one to account for the increased cross-sectional area of the columns. At this stage of the study, the sole environmental consequences were updated to check how this would influence the outcomes. All component quantities for each floor and direction and the corresponding fragility functions, for the as-built and concrete jacketing configurations, are reported in Table 1 and Figure 5, respectively. It is noted that two fictitious floors, 4.5 m and 1.5 m high, respectively, were assumed for those configurations to consider the potential damage of the short columns. Indeed, as shown in the following Table **1** and Table **2**, on the second "floor", only shorts-column components were numbered, while on first "floor" only exterior masonry infills without windows were included.

Floor	Component	*x* dir.	*y* dir.	Unit
1	Brittle columns	0	0	piece
	Exterior masonry infills without windows - out of plane	180	486	m^2
2	Brittle columns	20	20	piece
	Exterior masonry infills without windows - out of plane	0	0	m^2

Table 1: Building's components quantities for the as-built and concrete jacketing configurations.

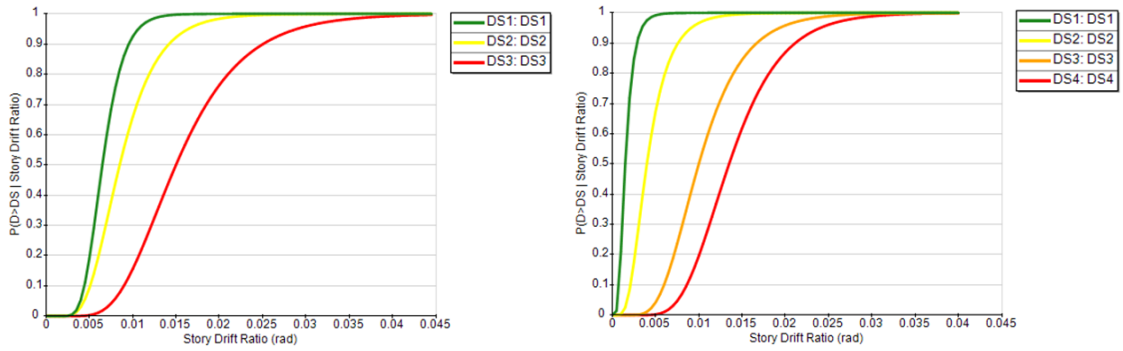

Figure 5: Fragility functions for (left) brittle columns (BWC) and (right) exterior masonry infills without windows (EIW).

Coming to the retrofitted configuration with energy dissipation devices, components representative of friction rotation dampers and diagonal steel braces with dissipative sacrificial elements were included. Namely, the fragility function developed by Nuzzo (2019) [25] for a shear link (SL) damper was used as a proxy for friction rotation dampers, in the lack of other more representative components. The damage state considered herein is associated to the attainment of the 75% of the damper's deformation capacity, something that leads to the replacement of

the damper. Such dampers were counted per piece in the *x* direction only. The fragility and repair cost functions of these components were taken from Nuzzo (2019) [25]. For repair costs, an inflation factor equals to 1.27 was applied to the original cost values, which were estimated according to 2016 Italian price list [25]. The consequence function in terms of equivalent carbon dioxide was instead defined by using the values of global warming potential (in kg of equivalent carbon dioxide, kg CO_2e) evaluated in [14] for replacing an individual friction rotation damper, as shown in Table 3.

For diagonal steel braces with dissipative sacrificial elements, special concentric braced frames were selected from the PACT [21][22] library, in the lack of other more suitable references in the literature. A single damage state, corresponding to initial stages of brace buckling, was identified as representative of the behaviour of braces with dissipative elements. The collapse of bracings is typically due to buckling, which in the configuration explored here is avoided thanks to the presence of sacrificial elements. The repair cost and embodied carbon functions of special concentric braced frames were thus modified to consider the exact quantities of the sole damageable parts, i.e. the sacrificial elements. All component quantities for each floor and direction and the corresponding fragility functions, for the retrofitted configuration with energy dissipation devices, are illustrated in Table 2 and Figure 6, respectively.

Floor	Component	*x* dir.	*y* dir.	Unit
1	Brittle columns	0	0	piece
	Exterior masonry infills without windows - out of plane	180	486	m^2
	Friction rotation dampers	0	0	piece
	Diagonal steel braces + dissipative sacrificial elements	0	2	piece
2	Brittle columns	20	20	piece
	Exterior masonry infills without windows - out of plane	0	0	m^2
	Friction rotation dampers	20	0	piece
	Diagonal steel braces + dissipative sacrificial elements	0	0	piece

Table 2: Building's components quantities for the retrofitted configuration with dissipation-based devices.

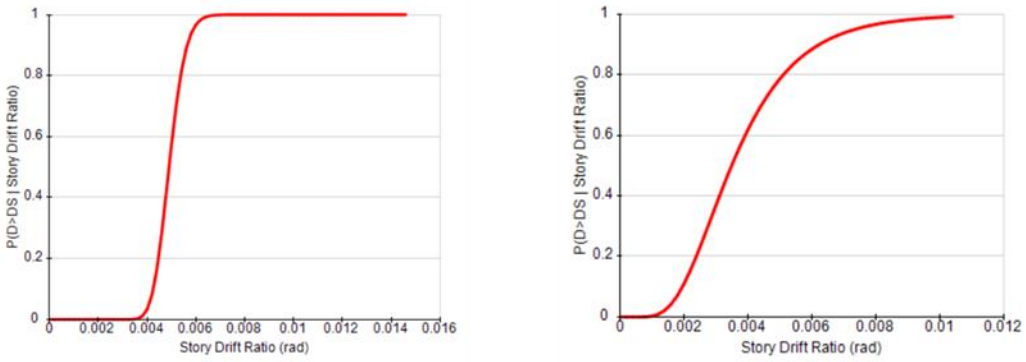

Figure 6: Fragility functions for (left) shear link (SL) damper and (right) diagonal steel braces with dissipative sacrificial elements.

Further information on the components used herein, including descriptions of damage states and corresponding repair activity, as well as repair costs and embodied carbon functions, can be found in Table 3. Repair cost functions are defined in terms of a maximum cost, associated to a lower quantity of components that need to be repaired, and a minimum cost, associated to an upper quantity of components, to consider economies of scale. Repair embodied carbon

functions, which are assumed to follow a lognormal distribution, are instead shown in terms of their median, in kg CO_2e.

As-built configuration

RC brittle weak columns (0.35x0.35 m)

Damage state	Description	Repair activity	Repair cost (€/unit)	Repair carbon (kg CO_2e/unit)
DS1	Light cracking.	Epoxy injection of concrete cracks.	1,466 – 2,387	102
DS2	Severe cracking, spalling of concrete cover.	Concrete patch with mortar mix.	3,069 – 4,331	200
DS3	Crushing of concrete, possible buckling of rebars.	Replace concrete and rebars if needed.	3,164 – 4,470	206

Exterior masonry infills without windows - out of plane

Damage state	Description	Repair activity	Repair cost (€/unit)	Repair carbon (kg CO_2e/unit)
DS1	Detachment of infill, light diagonal cracking.	Patch some cracks.	12 – 19	8
DS2	Extensive diagonal cracking, possible failure of brick units.	Patch cracks and restore loose masonry.	27 – 38	18
DS3	Corner crushing and sliding of mortar joints.	Demolish existing wall and construct a new wall. Re-install the existing frame if any.	127 – 181	83
DS4	Out-of-plane collapse.	Demolish existing wall and construct a new wall. Install a new frame if any.	130 – 182	84

Retrofit configuration with concrete jacketing of columns

RC brittle weak columns (0.55x0.55 m)

Damage state	Description	Repair activity	Repair cost (€/unit)	Repair carbon (kg CO_2e/unit)
DS1	Light cracking.	Epoxy injection of concrete cracks.	1,466 – 2,387	251
DS2	Severe cracking, spalling of concrete cover.	Concrete patch with mortar mix.	3,069 – 4,331	493
DS3	Crushing of concrete, possible buckling of rebars.	Replace concrete and rebars if needed.	3,164 – 4,470	508

Exterior masonry infills without windows - out of plane (same as above)

Retrofit configuration with energy dissipation devices

RC brittle weak columns (0.35x0.35 m) (same as above)

Exterior masonry infills without windows - out of plane (same as above)				
Friction rotation dampers				
Damage state	Description	Repair activity	Repair cost (€/unit)	Repair carbon (kg CO_2e/unit)
DS1	Attainment of the 75% of the damper's deformation capacity.	Replacement of the damper.	483 – 991	340
Diagonal steel braces with dissipative sacrificial elements				
Damage state	Description	Repair activity	Repair cost (€/unit)	Repair carbon (kg CO_2e/unit)
DS1	Initial stage of brace buckling and failure of sacrificial elements.	Replacement of the sacrificial elements present in the braces.	290 – 465	28

Table 3: Damage states and consequence functions for all building components used in the case study application.

For each of the three configurations, based on the MSA described in Section 3, the inter-storey drifts in *x* and *y* directions were extracted by dividing the relative displacements between the floors by the corresponding inter-storey height. Thus, for each of the ten IM levels, it was possible to obtain the seismic demand in terms of inter-storey drifts used in each fragility considered. Inter-storey drifts profiles were then collected in Pact for each intensity level and for both *x* and *y* directions, assuming 1,000 realisations and dispersions equal to 0.4 based on the model's characteristics. Furthermore, the buildings' collapse fragility functions were derived from the MSA, relating the probability of incurring structural collapse to ground motion intensity.

Additional assumptions for the calculation of seismic losses (step iv) are related to the total replacement economic and environmental costs of the building. These parameters were defined based on the assumption that, in case of collapse or non-repairable scenarios, both as-built and retrofitted building configurations would be replaced with a new building according to current (modern) construction techniques. The total replacement cost was estimated as equal to 594,000 €, by assuming a construction cost of 550 €/m^2 (based on discussions with practitioners) and a floor area of 1,080 m^2. The total replacement embodied carbon was evaluated as equal to 280,800 kg CO_2e, by assuming 260 kg CO_2e/m^2 (based on the authors' judgment). The total costs of each retrofit, i.e. 128,995 € for the jacketing solution and 51,186 € for the dissipative solution, represent 22% and 9% of the total replacement cost, respectively. On the other hand, the carbon embedded in each retrofit, i.e. 31,837.60 kg CO_2e for the jacketing solution and 11,878.22 kg CO_2e for the dissipative solution, represent 11% and 4% of the replacement embodied carbon, respectively.

Seismic losses resulting from the assessment are summarised in Table 4 for all configurations. The economic average annual loss ratio (AALR) and average annual embodied carbon ratio (AAECR) were obtained as fractions between loss curve integrals and total replacement values. Economic and environmental seismic losses are almost coincident for the two interventions, as it would be expected by adopting iso-performance retrofit design processes. However, it can be observed that the innovative retrofit provides slight economic advantages but not environmental ones, if compared to concrete jacketing.

	As-built	Concrete jacketing retrofit	Dissipation-based retrofit
Total replacement cost (€)	594,000	594,000	594,000
Repair cost (AAL: €/year)	1,842	1,071	1,024
$\text{AALR}\ (\frac{1}{\text{year}}) = \frac{\text{Repair cost}}{\text{Total replacement cost}}$	0.31%	0.18%	0.17%
Total replacement embodied carbon (kg CO_2e)	280,800	280,800	280,800
Repair embodied carbon (AAEC: kg CO_2e/year)	295	247	254
$\text{AAECR}\ (\frac{1}{\text{year}}) = \frac{\text{Repair embodied carbon}}{\text{Total replacement embodied carbon}}$	0.11%	0.088%	0.091%

Table 4: Seismic loss assessment results for all configurations.

On the other hand, by adopting some of the parameters considered in the multi-criteria decision-making approach proposed by Caruso et al. (2023) [11], it was possible to compare the as-built configuration and the retrofitted scenarios under a life cycle perspective, considering, namely: life cycle costs ($LCPM_€$), life cycle carbon emissions ($LCPM_{kg\ CO2e}$) and economic payback period ($PB_{econ.}$). The life cycle parameters $LCPM_€$ and $LCPM_{kg\ CO2e}$ were obtained by summing the economic and environmental costs of each retrofit and the corresponding seismic losses (AAL and AAEC), multiplied by the post-retrofit building life (assumed herein as 50 years), thus normalising the result by the total building floor area and the post-retrofit building life. The economic payback period ($PB_{econ.}$), instead, was calculated as the ratio between each retrofit cost and the corresponding economic savings (i.e. the difference between the as-built and retrofitted configurations seismic repair costs). All the results are summarised in Table 5.

	As-built	Concrete jacketing retrofit	Dissipation-based retrofit
$\text{LCPM €}\ (\frac{€}{\text{m}^2 * \text{year}}) = \frac{\text{Retrofit cost} + (\text{AAL} * 50\ \text{years})}{\text{floor area} * 50\ \text{years}}$	1.71	3.38	1.90
$\text{LCPM}_{\text{CO2e}}\ (\frac{\text{kg eCO}_2}{\text{m}^2 * \text{year}}) = \frac{\text{Retrofit embodied carbon} + (\text{AAEC} * 50\ \text{years})}{\text{floor area} * 50\ \text{years}}$	0.27	0.82	0.46
$\text{PB econ. (year)} = \frac{\text{Retrofit cost}}{\text{As–built Repair cost} - \text{Retrofit Repair cost}}$	0	167	63

Table 5: Life cycle parameters of the MCDM proposed by Caruso et al. (2023) for all configurations.

The $LCPM_{€}$ and $LCPM_{kg\ CO2e}$ parameters reported in Table 5 show that the innovative retrofit provides larger economic and environmental benefits under a life cycle perspective, resulting in around half of the impacts if compared to the concrete jacketing retrofit counterpart. It is worth noting that the as-built values are lower than the others, since they do not include the "initial" retrofit economic and environmental cost. Moreover, the calculation of the economic and environmental payback periods prove that the initial investment for the dissipation-based retrofit is expected to be amortised much faster than that for concrete jacketing.

5 CONCLUSIONS

Seismic rehabilitation is crucial to extend the nominal service life and help reduce the seismic losses of RC precast industrial buildings. This study discusses the potential reduction of the building earthquake-induced economic and environmental impacts through an application to a single-storey precast industrial building located in Naples. In previous work by the authors [14], two different retrofitting solutions, entailing concrete jacketing of columns and the use of two energy dissipation devices, respectively, were designed for the retrofit of the building at hand.

The retrofitted building configurations were herein compared by carrying out an assessment of the economic and environmental seismic losses, quantifying the AAL and the AAEC by the FEMA P-58 component-based approach [21][22]. This method demonstrated similar results, namely slight economic benefits for the innovative solution but not environmental ones, if compared to the traditional concrete jacketing. Subsequently, the impacts comparison was further conducted under a life cycle perspective, which proved larger economic and environmental advantages for the dissipation-based retrofitting solution. This work confirms the great potential of such innovative solution if compared to the more traditional concrete jacketing of columns.

6 ACKNOWLEDGEMENTS

This study was partially developed within the activities of the EUCENTRE-DPC 2022-2024 research program, which was funded by the Presidency of the Council of Ministers – Italian Civil Protection Department (DPC).

REFERENCES

[1] L. Praticò, M. Bovo, N. Buratti, M. Savoia, Large-scale seismic damage scenario assessment of precast buildings after the May 2012 Emilia earthquake. *Bulletin of Earthquake Engineering*, **20**(15), 8411-8444, 2022, https://doi.org/10.1007/s10518-022-01529-2.

[2] X. Li, G. Wu, Y.C. Kurama, H. Cui, Experimental comparisons of repairable precast concrete shear walls with a monolithic cast-in-place wall. *Engineering Structures*, **216**, 110671, 2020, https://doi.org/10.1016/j.engstruct.2020.110671.

[3] H. Guerrero, T. Ji, J.A. Escobar, A. Teran-Gilmore, Effects of buckling-restrained braces on reinforced concrete precast models subjected to shaking table excitation. *Engineering Structures*, **163**, 294-310, 2018, https://doi.org/10.1016/j.engstruct.2018.02.055.

[4] B. Dal Lago, M. Naveed, M. Lamperti Tornaghi, Tension-only ideal dissipative bracing for the seismic retrofit of precast industrial buildings. *Bulletin of Earthquake Engineering*, **19**(11), 4503-4532, 2021, https://doi.org/10.1007/s10518-021-01130-z.

[5] S. Santagati, D. Bellotti, D. Bolognini, E. Brunesi, Seismic response comparisons between RC precast structures with dissipation devices on beam-column connections. *15WCEE, 15th World Conference on Earthquake Engineering*, Lisbon, Portugal, September 24-28, 2012.

[6] A. Belleri, A. Marini, P. Riva, R. Nascimbene, Dissipating and re-centring devices for portal-frame precast structures. *Engineering Structures*, **15**, 736-745, 2017, https://doi.org/10.1016/j.engstruct.2017.07.072.

[7] M.M. Javidan, A. Ali, J. Kim, A steel hysteretic damper for seismic design and retrofit of precast portal frames. *Journal of Building Engineering*, **57**, 104958, 2022, https://doi.org/10.1016/j.jobe.2022.104958.

[8] D. Sonda, A.V. Pollini, TH analyses and simplified approach for precast RC frames retrofit with dissipative fuse devices Sismocell. *Procedia Structural Integrity*, **44**, 1188-1195, 2023, https://doi.org/10.1016/j.prostr.2023.01.153.

[9] G. Magliulo, M. Cimmino, M. Ercolino, G. Manfredi, Cyclic shear tests on RC precast beam-to-column connections retrofitted with a three-hinged steel device. *Bulletin of Earthquake Engineering*, **15**(9), 3797-3817, 2017, https://doi.org/10.1007/s10518-017-0114-x.

[10] C. Passoni, E. Palumbo, R. Pinho, A. Marini, The LCT challenge: defining new design objectives to increase the sustainability of building retrofit interventions, *Sustainability*, **14**(14), 8860, 2022, https://doi.org/10.3390/su14148860.

[11] M. Caruso, R. Pinho, F. Bianchi, F. Cavalieri, M.T. Lemmo, Multi-criteria decision-making approach for optimal seismic/energy retrofitting of existing buildings, *Earthquake Spectra*, **39**(1), 191-217, 2023, https://doi.org/10.1177/87552930221141917.

[12] N. Clemett, W. Carofilis, G. Gabbianelli, G.J. O'Reilly, R. Monteiro, Optimal combined seismic and energy efficiency retrofitting for existing buildings in Italy. *Journal of Structural Engineering*, **149**(1), 04022207, 2023, https://doi.org/10.1061/(ASCE)ST.1943-541X.0003500.

[13] L. Giresini, F. Stochino, M. Sassu, Economic vs environmental isocost and isoperformance curves for the seismic and energy improvement of buildings considering Life Cycle Assessment. *Engineering Structures*, **233**, 111923, 2021, https://doi.org/10.1016/j.engstruct.2021.111923.

[14] F. Cavalieri, D. Bellotti, M. Caruso, R. Nascimbene, Comparative evaluation of seismic performance and environmental impact of traditional and dissipation-based retrofitting solutions for precast structures. *Journal of Building Engineering*, **79**, 107918, 2023, https://doi.org/10.1016/j.jobe.2023.107918.

[15] Decreto Ministeriale 17/01/2018. *Aggiornamento delle "Norme tecniche per le costruzioni"*. In Suppl. ord. n. 8 alla G.U. Serie Generale n. 42 del 20/02/2018 (in Italian); Ministero delle Infrastrutture e dei Trasporti: Rome, Italy, 2018.

[16] Resilio system, Patent. Engineering company Astico Brenta, Thiene (Vicenza), Italy, 2017. Available online: https://www.sistemiresilienti.it/resilio-la-differenza/ (in Italian).

[17] F. McKenna, G.L. Fenves, M.H. Scott, *OpenSees: Open System for Earthquake Engineering Simulation*. University of California, Berkeley, CA, USA, 2000. Available online: http://opensees.berkeley.edu.

[18] RINTC, *Implicit seismic risk of code-conforming structures in Italy*, Joint project ReLUIS and EUCENTRE, funded by the Italian Department of Civil Protection (DPC), 2022-2024.

[19] F. Jalayer, C.A. Cornell, Alternative non-linear demand estimation methods for probability-based seismic assessments. *Earthquake Engineering & Structural Dynamics*, **38**(8), 951-972, 2009, https://doi.org/10.1002/eqe.876.

[20] L. Luzi, G. Lanzano, C. Felicetta, M.C. D'Amico, E. Russo, S. Sgobba, F. Pacor, *ORFEUS Working Group 5, Engineering Strong Motion Database (ESM) (Version 2.0)*. Istituto Nazionale di Geofisica e Vulcanologia (INGV). Available online: https://esm-db.eu/#/home, 2020.

[21] Applied Technology Council (ATC), *Seismic Performance Assessment of Buildings—Methodology (Rep No FEMA P-58-1), vol. 1*, Federal Emergency Management Agency (FEMA), Washington, DC, 2018a.

[22] Applied Technology Council (ATC), *Seismic Performance Assessment of Buildings—Implementation Guide (Rep No FEMA P-58-2), vol. 2*, Federal Emergency Management Agency (FEMA), Washington, DC, 2018b.

[23] D. Cardone, Fragility curves and loss functions for RC structural components with smooth rebars. *Earthquakes and Structures*, **10**(5), 1181-1212, 2016, http://dx.doi.org/10.12989/eas.2016.10.5.1181.

[24] D. Cardone, G. Perrone, Developing fragility curves and loss functions for masonry infill walls. *Earthquakes and Structures*, **9**(1), 257-279, 2015, https://doi.org/10.12989/eas.2015.9.1.257.

[25] I. Nuzzo, Case-study of a cost-based seismic design for a R.C. frame with additional dissipative brace systems. M. Papadrakakis, M. Fragiadakis (eds.), *COMPDYN 2019, 7th ECCOMAS Thematic Conference on Computational Methods in Structural Dynamics and Earthquake Engineering*, Crete, Greece, June 24-26, 2019, 10.7712/120119.7152.19266.